Bioorganic & Medicinal Chemistry Letters 21 (2011) 2255–2258

Contents lists available at ScienceDirect

Bioorganic & Medicinal Chemistry Letters

journal homepage: www.elsevier.com/locate/bmcl

3,5-Disubstituted-indole-7-carboxamides: The discovery of a novel series of potent, selective inhibitors of IKK-β

David D. Miller [a], Paul Bamborough [a,*], John A. Christopher [a], Ian R. Baldwin [a], Aurelie C. Champigny [a], Geoffrey J. Cutler [a], Jeffrey K. Kerns [b], Timothy Longstaff [a], Geoffrey W. Mellor [a], James V. Morey [a], Mary A. Morse [a], Hong Nie [b], William L. Rumsey [b], John J. Taggart [b]

[a] GlaxoSmithKline R&D, Medicines Research Centre, Gunnels Wood Road, Stevenage, Hertfordshire SG1 2NY, UK
[b] GlaxoSmithKline Inc., 709 Swedeland Road, King of Prussia, PA 19406, USA

ARTICLE INFO

Article history:
Received 2 February 2011
Revised 24 February 2011
Accepted 25 February 2011
Available online 1 March 2011

Keywords:
Kinase
IKK-β
IKK
Indolecarboxamide

ABSTRACT

The discovery and hit-to-lead exploration of a novel series of selective IKK-β kinase inhibitors is described. The initial lead fragment **3** was identified by pharmacophore-directed virtual screening. Homology model-driven SAR exploration of the template led to potent inhibitors, such as **12**, which demonstrate efficacy in cellular assays and possess encouraging developability profiles.

Protein kinases are regulators of a broad range of cellular processes. Consequently, kinases involved in disease-associated aberrant signalling are considered attractive targets for drug discovery. IκB kinase β (IKK-β or IKK-2) is a serine/threonine kinase located on an isolated branch of the kinase phylogenetic tree along with 3 homologous family members, IKK-α (IKK-1), IKK-ε (IKK-3) and TBK1 (IKK-4).[1] Ubiquitously expressed, IKK-β is a member of the IKK signalsome which regulates the signalling pathway that links cellular engagement of pro-inflammatory stimuli such as lipopolysaccharide (LPS) and tumour necrosis factor-α (TNF-α) to the transcription factor Nuclear Factor kappa B (NF-κB).[2] Phosphorylation by IKK-β of IκB (inhibitor of kappa B) in a cytosolic complex with NF-κB leads to the ubiquitination and proteosomal degradation of IκB. This releases NF-kB and allows it to translocate to the nucleus, where it regulates the expression of multiple genes, leading to a range of immune and inflammatory responses.[2,3] IKK-β inhibition alone is believed to be sufficient to block the activation of NF-κB[4] and as a result the search for small-molecule inhibitors of IKK- β as drugs for use in the control of NF-κB-associated diseases such as asthma, COPD and rheumatoid arthritis has attracted much attention.[5–8]

Here, we describe the discovery and preliminary SAR of a series of indole-7-carboxamide IKK-β inhibitors that were identified through the application of pharmacophore-directed database searches. The objective in the lead discovery phase was to find novel IKK-β inhibitor templates that would meet the minimum target profile described in Figure 1 and, in addition, have suitable drug-like properties to provide confidence to initiate a lead optimization programme. Although IKK-α (IKK-1), which is also found in the IKK signalsome, is reported to be much less active as a kinase than IKK-β,[9] it has been reported to have non-redundant roles in signalling[10] and so IKK-β inhibitors with selectivity over IKK-α were sought as a complement to dual-active compounds.[11]

In vitro potency	$pIC_{50} > 6.5$
Selectivity	>10 fold over IKK-α
Cellular potency	$pIC_{50} > 5.7$ in relevant cells

Figure 1. Minimum target lead profile; $pIC_{50} = -(\log_{10} IC_{50})$.

In the absence of crystallographic data on IKK-β, a 3D pharmacophore was built from a homology model based on the X-ray structure of CDK2 complexed with **1**, a close analogue of a literature thiophene carboxamide IKK-β inhibitor TPCA-1 (Fig. 2).[12,13]

A 3D pharmacophore search of the GSK screening collection (Fig. 2) identified several hundred compounds which were tested for IKK-β inhibition. From this, a small number of weakly active hits containing the motifs shown in Figure 3 were identified. These results contributed to the observation that a variety of IKK-β inhibitors contain a primary carboxamide held in a constrained conformation by an adjacent hydrogen-bonding functionality. A separate

* Corresponding author. Tel.: +44 1438 763246.
E-mail address: paul.a.bamborough@gsk.com (P. Bamborough).

0960-894X/$ - see front matter © 2011 Elsevier Ltd. All rights reserved.
doi:10.1016/j.bmcl.2011.02.107

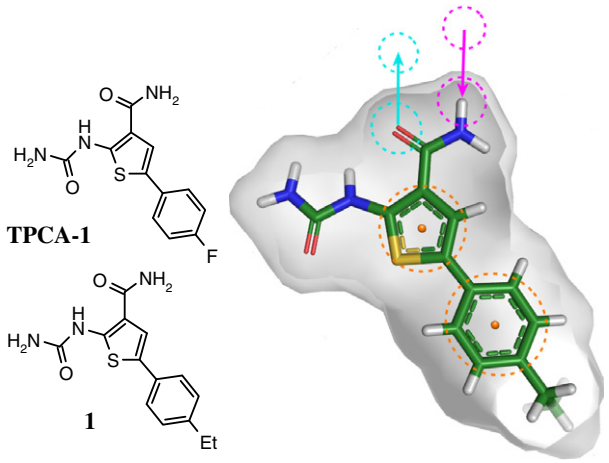

Figure 2. IKK-β pharmacophore based on X-ray complex between thiophene carboxamide **1** (IKK-β pIC_{50} 8.1) and CDK2. Aromatic centroid (orange) and H-bond donor (magenta) and acceptor (cyan) vectors are shown.

Figure 3. Frequently occurring motifs observed in preliminary hits.

exercise subsequently exploited this to find inhibitors of both IKK-α and IKK-β kinases.[11]

A substructure search based on the these motifs led to the testing in the IKK-β enzyme assay of tricyclic indole derivative **2** (Fig. 4), which was found to be modestly active.[14] Compound **2** resembles another series of β-carboline IKK-β inhibitors.[15] Since the β-carbolines do not contain the primary carboxamide motif essential for the activity of the indole carboxamides (see later, Fig. 6) we believe them to be distinct.

SAR knowledge from the thiophene series (e.g. TPCA-1) suggested that the cyclohexene ring could be removed and that the bromine in the 5-position could be replaced by other groups such as aryl rings. Carrying out these changes did indeed produce a lead compound **3** that retained potency at IKK-β in the micromolar range. **3** has high ligand efficiency, low molecular weight and low lipophilicity (LE = 0.44, MW = 236, *c* Log *P* = 2.7).[16]

The route devised for the synthesis of **3** and related analogues is described in Scheme 1.[17] Boc protection of indoline **4** followed by lithiation and quenching with methyl chloroformate provided the protected, carboxylated indoline **5** which was brominated, Boc-deprotected, oxidised to the indole and the ester saponified to give the key, versatile intermediate **6**. Conversion to the primary amide and di-protection yielded **7**, which was used as a substrate in a

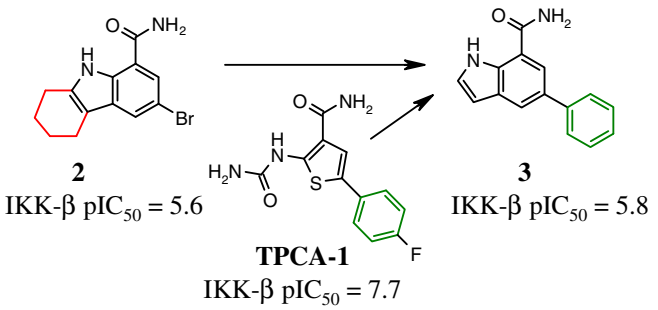

Figure 4. Initial lead compounds.

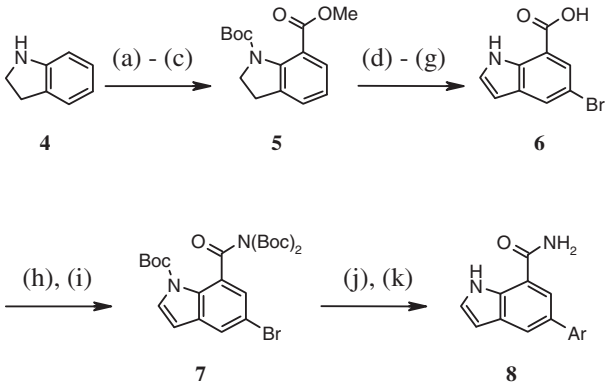

Scheme 1. Reagents and conditions: (a) Boc_2O, THF, rt; (b) *s*-BuLi, TMEDA, THF, −78 °C; (c) ClC(O)OMe, −78 °C; (d) NBS, CH_2Cl_2, rt; (e) TFA, rt; (f) MnO_2, THF, rt; (g) LiOH, MeOH, Δ; (h) NH_3/dioxane, HATU, DIPEA, CH_2Cl_2 rt; (i) Boc_2O, DMAP, CH_2Cl_2 rt; (j) $ArB(OH)_2$, K_2CO_3, $PdCl_2(dppf)$, CH_2Cl_2, DMF, 80 °C; (k) cHCl, EtOH, μ-wave, 150 °C, 5 min.

series of palladium-catalysed arylation reactions followed by deprotection to the target compounds **8**.

Preliminary exploration of the SAR around the template indicated that a variety of groups was tolerated at the 5-position of the indole (Table 1). With a substituted phenyl group in this position, potency at IKK-β generally increased in the order *ortho* < *meta* < *para* (e.g., **8c**–**8e**) and the promising selectivity over IKK-α improved between *meta* and *para* (cf. **8d** with **8e** and **8f** with **8g**). Early indications suggested that heterocycles could also be accommodated in this position (**8h**–**8j**). These results provided confidence that there would be significant scope for modulation of potency and compound properties through variation at the 5-position of the indole during lead optimisation.

Docking of structure **3** into the IKK-β homology model predicted a binding mode that is consistent with that of thiophene **1** in the X-ray complex with CDK-2. The carboxamide forms hydrogen-bonds to Glu97 and Cys99 of the kinase hinge region and the indole NH holds the carboxamide co-planar with the indole via a further intramolecular hydrogen-bond (Fig. 5).[13]

The binding hypothesis was supported by the observation that compounds **9** and **10**, which were made by variation of the route described in Scheme 1 and which were expected to be unable to bind in the predicted manner, were both undetectable in the IKK-β assay (Fig. 6).

A further attraction of the indole core as a potential lead template was the access it offered from its 3-position to regions of the IKK-β active site that were not accessible from the corresponding position of thiophene-based inhibitors such as **1** because of the position of the sulphur atom. The key protein residues that were

Table 1
IKK-β and IKK-α inhibition by compounds **3** and **8a**–**j**[14]

Compounds	Ar	IKK-β pIC_{50}[a]	IKK-α pIC_{50}[a]
3	Ph	5.8	5.0
8a	3-CN-Ph	5.8	5.0
8b	4-$MeSO_2NH$-Ph	6.3	5.4
8c	2-Cl-Ph	5.2	<4.8
8d	3-Cl-Ph	6.1	5.3
8e	4-Cl-Ph	6.5	5.2
8f	3-$HOCH_2$-Ph	5.6	4.8
8g	4-$HOCH_2$-Ph	5.9	4.8
8h	5-Pyrimidinyl	5.3	4.8
8i	4-Methoxy-3-Pyridinyl	5.8	4.9
8j	2-Benzofuranyl	6.3	5.4

[a] Values are means of at least two replicates.

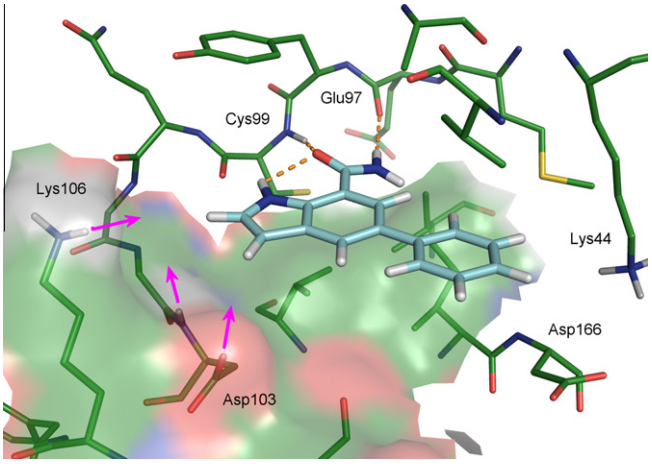

Figure 5. Compound **3** docked into IKK-β homology model. Magenta arrows indicate vectors for hydrogen-bonding to Asp103 and Lys106.

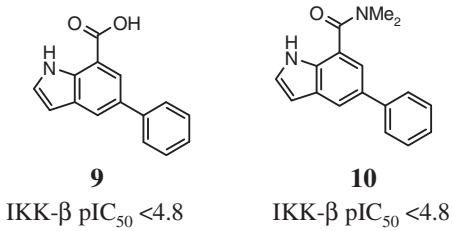

9 IKK-β pIC_{50} <4.8

10 IKK-β pIC_{50} <4.8

Figure 6. Modifications predicted not to bind to kinase hinge.

targeted were Asp103 and Lys106 (Fig. 5). The first substitutents explored at the indole 3-position were 3- and 4-piperidyl groups (Scheme 2). These were included because of the predicted binding mode of compound **11**, a literature 2-hydroxy pyridin-2-yl IKK-β inhibitor with a reported IC_{50} of 25 nM.[18] In its presumed binding mode, compound **11** accepts the hinge hydrogen-bond from Cys99 using its phenolic oxygen, while the 3-piperidine group forms a charged hydrogen-bonding interaction with the sidechain of Asp103.

Condensation of **3** with *N*-benzyl -3-piperidone or -4-piperidone followed by simultaneous reduction and deprotection of the

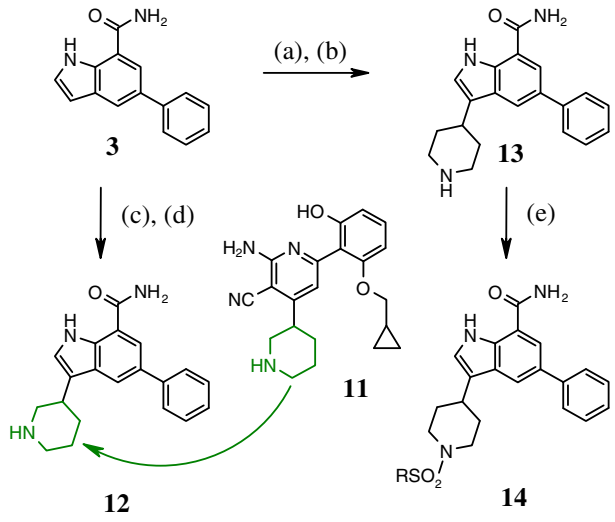

Scheme 2. Reagents and conditions: (a) *N*-benzyl-4-piperidone, MeONa, MeOH, Δ; (b) $Pd(OH)_2/C$, H_2, EtOH/AcOH, rt; (c) *N*-benzyl-3-piperidone·HCl, KOH, MeOH, Δ; (d) $Pd(OH)_2/C$, H_2, EtOH, rt; (e) RSO_2Cl, pyridine, rt.

Table 2
Enzyme inhibition by 3-substituted compounds **12–14**[14]

Compds	R	IKK-β pIC_{50}[a]	IKK-α pIC_{50}[a]	IKK-β LE[16]
3	—	5.8	5.0	0.44
12	—	6.8	5.8	0.39
13	—	6.3	5.0	0.36
14a	$nPrSO_2$	7.9	5.7	0.36
14b	$iPrSO_2$	7.7	5.5	0.35
14c	$EtSO_2$	7.6	5.7	0.36
14d	4-Cl-$PhSO_2$	6.4	5.1	0.26

[a] Values are means of at least two replicates.

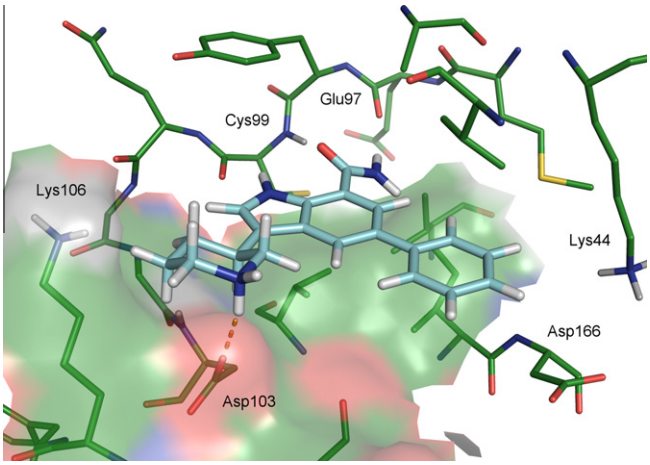

Figure 7. Compound **12** docked into IKK-β homology model highlighting the putative interaction with Asp103.

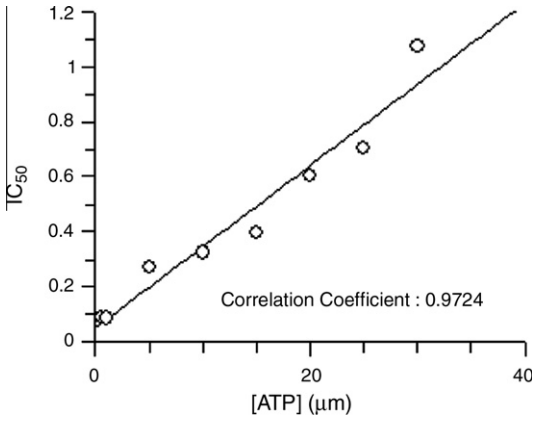

Figure 8. ATP concentration dependent IKK-β inhibition by **12**.

resulting benzyltetrahydropyridine intermediate yielded the 3-piperidyl and 4-piperidyl products **12** and **13** respectively.

The superior potency of **12** in inhibiting IKK-β (Table 2) is attributed to the formation of a similar charged pair interaction between the protonated nitrogen of the piperidine and the carboxylate side chain of Asp103, as shown in Figure 7.

A detailed analysis of the enzyme inhibition kinetics for **12** through IC_{50} measurement across a range of ATP concentrations showed an ATP concentration dependent inhibition of IKK-β, consistent with the compound having an ATP-competitive mode of action (Fig. 8).

A further, significant increase in IKK-β inhibitory potency was achieved though conversion of the 4-piperidyl derivative **13** into certain sulphonamides (e.g., **14a–d**). This increase was anticipated

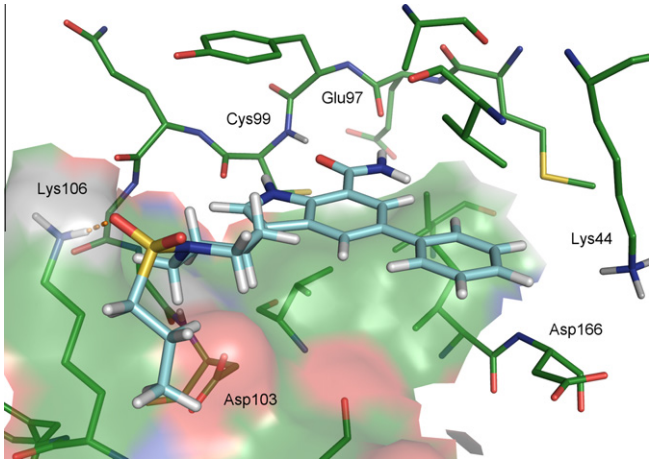

Figure 9. Compound **14a** docked into IKK-β homology model highlighting the putative interaction with Lys106.

by docking studies which predicted that modifying the nitrogen to an uncharged sulphonamide could permit hydrogen-bonding between an oxygen of the sulphonamide and the side-chain NH_3^+ of Lysine 106 or the backbone NH of Asp103 (Fig. 9).

Very promisingly, the enzyme inhibition of compounds **12** and **14a** translated into cellular efficacy in an assay measuring the compounds' ability to inhibit the LPS stimulated production of TNF-α in peripheral blood mononuclear cells (PBMC), each inhibiting with a pIC_{50} of 6.2.[19] Furthermore, compound **14a** was found to inhibit NF-κB translocation in TNF-α treated A549 cells potently, with a pIC_{50} of 6.8.[19]

Wider selectivity screening across an in-house panel of >45 kinase assays showed an excellent profile for compounds **12** and **14a**. Both compounds had pIC_{50} <5.5 across the entire panel, which included IKK-ε and TBK1, with the following exceptions: **12**, BTK pIC_{50} = 5.9 and c-FMS pIC_{50} = 5.8; and **14a**, BTK pIC_{50} = 5.8 and Aurora A pIC_{50} = 5.9. In addition, **14a** was screened at 10 μM against a panel of 105 kinases in a binding format.[20] Where binding was detected the K_d was determined. Only two kinases gave pK_d > 5.5 (CSNK1ε, pK_d = 5.8, and FLT3 pK_d = 5.9).

In addition to the excellent IKK-β and broader kinase profile observed in the series, exemplars also displayed favourable developability characteristics. For example, compound **12** had high aqueous solubility (136 μg/ml), low protein binding (91% to Human Serum Albumin), low in vitro clearance (human <1 ml/min/mg) and encouraging oral bioavailability (22% in rat).

In summary, pharmacophore directed screening was used to identify a novel IKK-β inhibitor fragment template. Homology model-based SAR exploration led to the discovery of potent, selective inhibitors with cellular efficacy. Key exemplars such as **12** and **14a** exceeded the minimum target profile and preliminary DMPK data and wider profiling augured well for further optimisation of this new class of IKK-β inhibitors, which will be described in future publications.

Acknowledgements

The authors gratefully acknowledge Duncan Judd for technical support in the provision of scaled-up quantities of key synthetic intermediates, Lisa Shewchuk for obtaining the crystal structure of **1** in CDK2, and all the members of the IKK-β team.

References and notes

1. Manning, G.; Whyte, D. B.; Martinez, R.; Hunter, T.; Sudarsanam, S. *Science* **2002**, *298*, 1912.
2. Karin, M.; Yamamoto, Y.; Wang, Q. M. *Nat. Rev. Drug Disc.* **2004**, *3*, 17.
3. Pahl, H. L. *Oncogene* **1999**, *18*, 6853.
4. Hacker, H.; Karin, M. *Sci. STKE.* **2006**, *357*, re13.
5. Coish, D. G.; Wickens, P. L.; Lowinger, T. B. *Expert Opin. Ther. Patents* **2006**, *16*, 1.
6. Pitts, W. J.; Kempson, J. *Annu. Rep. Med. Chem.* **2008**, *43*, 155.
7. Bamborough, P.; Callahan, J. F.; Christopher, J. A.; Kerns, J. K.; Liddle, J.; Miller, D. D.; Morse, M. A.; Rumsey, W. L.; Williamson, R. *Curr. Topics Med. Chem.* **2009**, *9*, 623.
8. Bamborough, P.; Morse, M. A.; Ray, K. P. *Drug News Perspect.* **2010**, *23*, 483.
9. Li, J.; Peet, G. W.; Pullen, S. S.; Shembri-King, J.; Warren, T. C.; Marcu, K. B.; Kehry, M. R.; Barton, R.; Jakes, S. *J. Biol. Chem.* **1998**, *273*, 30736.
10. Bonizzi, G.; Karin, M. *Trends Immunol.* **2004**, *25*, 280.
11. Christopher, J. A.; Avitable, B. G.; Bamborough, P.; Champigny, A. C.; Cutler, G. J.; Dyos, S. L.; Grace, K. G.; Kerns, J. K.; Kitson, J. D.; Mellor, G. W.; Morey, J. V.; Morse, M. A.; O'Malley, C. F.; Patel, C. B.; Probst, N.; Rumsey, W.; Smith, C. A.; Wilson, M. J. *Bioorg. Med. Chem. Lett.* **2007**, *17*, 3972.
12. Podolin, P. L.; Callahan, J. F.; Bolognese, B. J.; Li, Y. H.; Carlson, K.; Davis, T. G.; Mellor, G. W.; Evans, C.; Roshak, A. K. J. *J. Pharmacol. Exp. Ther.* **2005**, *312*, 373.
13. Homology modelling, pharmacophore searching and docking were carried out as described in Ref. 11.
14. IKK-β kinase inhibitory activity was determined using a time-resolved fluorescence resonance energy transfer (TR-FRET) assay. Recombinant GST-tagged human IKK-β (1-737) (typically 2–5 nM final) diluted in assay buffer (50 mM HEPES, 10 mM $MgCl_2$, 1 mM CHAPS pH 7.4 with 1 mM DTT and 0.01% w/v BSA) was added to wells containing compound or DMSO vehicle (less than 5% final). The reaction was initiated by the addition of GST-IκBα substrate (25 nM final)/ATP (1 μM final), in a total volume of 6 μl. IKK-α kinase inhibitory activity was determined similarly, using 6-His-tagged full length IKK-α. For further details see Ref.[11]. The error within both assays is estimated as ±0.3 log units, based on the standard deviation around the mean value of an inhibitor used as a standard compound in every assay.
15. Castro, A. C.; Dang, L. C.; Soucy, F.; Grenier, L.; Mazdiyasni, H.; Hottelet, M.; Parent, L.; Pien, C.; Palombella, V.; Adams, J. *Bioorg. Med. Chem. Lett.* **2003**, *13*, 2419.
16. See discussion by Abad-Zapatero, C. *Expert Opin. Drug Disc.* **2007**, *2*, 469. Ligand Efficiency $LE = -RT(\ln K_i)/N$, where N = number of heavy atoms. Here this is approximated for relative comparision by exchanging IC_{50} for K_i.
17. Baldwin, I. R.; Bamborough, P.; Christopher, J. A.; Kerns, J. K.; Longstaff, T.; Miller, D. D. WO 2005/067923.
18. Murata, T.; Shimada, M.; Kadono, H.; Sakakibara, S.; Yoshino, T.; Masuda, T.; Shimazaki, M.; Shintani, T.; Fuchikami, K.; Bacon, K. B.; Ziegelbauer, K. B.; Lowinger, T. B. *Bioorg. Med. Chem. Lett.* **2004**, *14*, 4013.
19. Details of the PBMC and NF-κB cellular assays are described in Bamborough, P.; Barker, M. D.; Campos, S. A.; Cousins, R. P. C.; Faulder, P.; Hobbs, H.; Holmes, D. S.; Johnston, M. J.; Liddle, J.; Payne, J. J.; Pritchard, J. M.; Whitworth, C. WO 2008/034860.
20. The ability of compounds at 10 μM concentration to displace kinases from immobilized ATP-site probe ligands was determined as previously described, see: Fabian, M. A.; Biggs, W. H., III; Treiber, D. K.; Atteridge, C. E.; Azimioara, M. D.; Benedetti, M. G.; Carter, T. A.; Ciceri, P.; Edeen, P. T.; Floyd, M.; Ford, J. M.; Galvin, M.; Gerlach, J. L.; Grotzfeld, R. M.; Herrgard, S.; Insko, D. E.; Insko, M. A.; Lai, A. G.; Lélias, J.-M.; Mehta, S. A.; Milanov, Z. V.; Velasco, A. M.; Wodicka, L. M.; Patel, H. K.; Zarrinkar, P. P.; Lockhart, D. J. *Nat. Biotechnol.* **2005**, *23*, 329.